PROCEEDINGS OF SCIENCE

Orbital Angular Momentum at Small x Revisited

Brandon Manley*

Department of Physics, The Ohio State University,
Columbus, OH U.S.A.

E-mail: manley.329@osu.edu

We revisit the the quark and gluon orbital angular momentum (OAM) distributions in the proton at small x. Utilizing the revised small-x helicity evolution from [1], we calculate the quark and gluon OAM distributions at small x, and relate them to the polarized dipole amplitudes and their (first) impact-parameter moments. To obtain the small-x asymptotics of the OAM distributions, we derive novel small-x evolution equations for the impact-parameter moments of the polarized dipole amplitudes in the double-logarithmic approximation (summing powers of $\alpha_s \ln^2(1/x)$ with α_s the strong coupling constant). We solve these evolution equations numerically and extract the large-N_c, small-x asymptotics of the quark and gluon OAM distributions, which we determine to be

$$L_{q+\bar{q}}(x,Q^2) \sim L_G(x,Q^2) \sim \Delta\Sigma(x,Q^2) \sim \Delta G(x,Q^2) \sim \left(\frac{1}{x}\right)^{3.66\sqrt{\frac{\alpha_s N_c}{2\pi}}},$$

in agreement with [2] within the precision of our numerical evaluation (here N_c is the number of quark colors). We also investigate the ratios of the quark and gluon OAM distributions to their helicity distribution counterparts in the small-x region.

25th International Spin Physics Symposium (SPIN 2023)
24-29 September 2023
Durham, NC, USA

*Speaker

PoS(SPIN2023)183

1. Introduction

These proceedings are based on [3], where we present this work in more detail.

The total spin of the proton comes from both the spin and orbital angular momentum (OAM) of its constituent quarks and gluons. This fact is quantified by spin sum rules. Here we consider the Jaffe-Manohar sum rule [4],

$$S_{q+\bar{q}}(Q^2) + L_{q+\bar{q}}(Q^2) + S_G(Q^2) + L_G(Q^2) = \frac{1}{2}, \tag{1}$$

where $S_{q+\bar{q}}$ and S_G are the quark and gluon spin angular momentum contributions, respectively. These contributions can be expressed as integrals over the helicity parton distribution functions (PDFs),

$$S_{q+\bar{q}}(Q^2) = \frac{1}{2}\int_0^1 dx\, \Delta\Sigma(x, Q^2), \qquad S_G(Q^2) = \int_0^1 dx\, \Delta G(x, Q^2), \tag{2a}$$

where $\Delta\Sigma(x, Q^2)$ is the quark flavor singlet helicity PDF and $\Delta G(x, Q^2)$ is the gluon helicity PDF.

$L_{q+\bar{q}}$ and L_G are the quark and gluon OAM contributions, respectively. All four contributions depend on the renormalization scale Q^2. The OAM contributions can also be expressed as integrals over distributions in the Bjorken-x variable,

$$L_{q+\bar{q}}(Q^2) = \int_0^1 dx\, L_{q+\bar{q}}(x, Q^2), \qquad L_G(Q^2) = \int_0^1 dx\, L_G(x, Q^2). \tag{3}$$

Particularly important for study is the small-x region of the integrals in Eqs. (3). This is because x scales with the inverse center of mass energy of the system. Therefore, experiments can only probe x down to some $x_{\min} > 0$. Theoretical input is needed for the region where $x < x_{\min}$. In this work, we address this problem by determining the small-x behavior of the OAM distributions $L_{q+\bar{q}}(x, Q^2)$ and $L_G(x, Q^2)$[1]. In Section 2, we utilize the dipole formalism at small x to relate the OAM distributions to the polarized dipole amplitudes and their first impact-parameter moments ("moment amplitudes"). Since the revised helicity evolution of [1] does not directly apply to the moment amplitudes, in Section 3, we construct their small-x evolution equations. In Section 4 we solve these evolution equations numerically and determine the small-x asymptotics of the OAM distributions. Additionally in Section 4 we investigate the ratios of the OAM distributions to their helicity counterparts in the small-x region. We conclude in Section 5.

2. OAM Distributions at Small x

Using Wigner functions $W(k, b)$, we can express the OAM distributions as [5–8]

$$L_z(Q^2) = \int \frac{d^2b_\perp db^- d^2k_\perp dk^+}{(2\pi)^3} \left(\underline{b} \times \underline{k}\right) W(k, b). \tag{4}$$

We denote the light-cone components of four-vectors by $x^\pm = (x^0 \pm x^3)/\sqrt{2}$ while transverse vectors are given as $\underline{x} = (x^1, x^2)$ with $\underline{x}_{ij} = \underline{x}_i - \underline{x}_j$ and $|\underline{x}_{ij}| = x_{ij}$ for i, j labeling the partons. We can extract the quark and gluon Wigner functions from the expressions for the unpolarized quark and

[1] This work is performed outside the saturation region.

gluon transverse momentum dependent distributions (TMDs) in a longitudinally polarized proton [8–10].

For the quark SIDIS process and the gluon dipole distribution, the quark and gluon Wigner functions are [8]

$$W^{\text{SIDIS}}_{q+\bar{q}}(k,b) = 2\sum_X \int dr^-\, d^2r_\perp\, e^{ik\cdot r}\left\langle \bar{\psi}\left(b-\frac{1}{2}r\right) V_{\underline{b}-\frac{1}{2}\underline{r}}\left[b^- - \frac{1}{2}r^-,\infty\right]|X\rangle \right. \tag{5a}$$
$$\left. \times \left(\frac{\gamma^+}{2}\right)\langle X|V_{\underline{b}+\frac{1}{2}\underline{r}}\left[\infty, b^- + \frac{1}{2}r^-\right]\psi\left(b+\frac{1}{2}r\right)\right\rangle,$$

$$W^{\text{dipole}}_G(k,b) = \frac{4}{xP^+}\int dr^-\, d^2r_\perp\, e^{ixP^+r^- - i\underline{k}\cdot\underline{r}} \tag{5b}$$
$$\times\left\langle \text{tr}\left[F^{+i}\left(b-\frac{1}{2}r\right)\mathcal{U}^{[+]}\left[b-\frac{1}{2}r, b+\frac{1}{2}r\right]F^{+i}\left(b+\frac{1}{2}r\right)\mathcal{U}^{[-]}\left[b+\frac{1}{2}r, b-\frac{1}{2}r\right]\right]\right\rangle,$$

where $k^+ = xP^+$ for P^+ the large proton momentum. $\mathcal{U}^{[+]}$ and $\mathcal{U}^{[-]}$ are the future and past pointing Wilson line staples, respectively.

We take our projectile to be moving along the x^- direction while our proton moves along the x^+ direction. We denote averaging in the proton's wavefunction by large brackets. Fundamental Wilson lines along the light-cone are denoted as

$$V_{\underline{x}}[b^-,a^-] = \mathcal{P}\exp\left[ig\int_{a^-}^{b^-} dx^- A^+(x^+=0,x^-,\underline{x})\right], \tag{6}$$

with $V_{\underline{x}} \equiv V_{\underline{x}}[\infty,-\infty]$ denoting infinite Wilson lines. Here g is the strong coupling constant and $A^\mu(x) = \sum_a A^{\mu\,a}(x)t^a$, with t^a the SU(N) generators.

In the dipole formalism, we treat the projectile as a dipole with $\underline{x}_0, \underline{x}_1$ denoting the transverse positions of the quark and antiquark. The softer parton has momentum fraction z. At the sub-eikonal (suppressed by one power of center-of-mass energy) level requisite for spin-dependent scattering [11], there are two types of polarized dipole amplitudes [1],

$$Q_{10}(zs) = \frac{zs}{2N_c}\text{Re}\left\langle \text{T tr}\left[V_{\underline{x}_0}\left(V^{\text{pol}[1]}_{\underline{x}_1}\right)^\dagger\right] + \text{T tr}\left[V^{\text{pol}[1]}_{\underline{x}_1}V^\dagger_{\underline{x}_0}\right]\right\rangle, \tag{7a}$$

$$G^i_{10}(zs) = \frac{zs}{2N_c}\text{Re}\left\langle \text{T tr}\left[V^\dagger_{\underline{x}_0}V^{i\,G[2]}_{\underline{x}_1}\right] + \text{T tr}\left[\left(V^{i\,G[2]}_{\underline{x}_1}\right)^\dagger V_{\underline{x}_0}\right]\right\rangle, \tag{7b}$$

where s is the dipole-target center of mass energy. The polarized Wilson lines, $V^{\text{pol}[1]}_{\underline{x}_1}$ and $V^{i\,G[2]}_{\underline{x}_1}$, represent sub-eikonal corrections to the quark propagator through the shockwave. Their operator definitions, along with the complete set of sub-eikonal corrections to the quark and gluon propagators through the shockwave can be found in [1].

Inspecting Eq. (4), it appears more convenient to work with impact-parameter integrated quantities. Integrating Eqs. (7) over all impact-parameters we get

$$\int d^2x_1\, Q_{10}(zs) = Q(x^2_{10}, zs), \tag{8a}$$

$$\int d^2x_1\, G^i_{10}(zs) = \epsilon^{ij}x^j_{10}\, G_2(x^2_{10}, zs) + \ldots. \tag{8b}$$

In addition to these impact-parameter integrated polarized dipole amplitudes, the angular momentum factor, $(\underline{b}\times\underline{k})$, in Eq. (4) means we also need the first impact-parameter moments of Eqs. (7),

$$\int d^2x_1\, x_1^i Q_{10}(zs) = x_{10}^i\, I_3(x_{10}^2, zs) + \dots, \tag{9a}$$

$$\int d^2x_1\, x_1^i G_{10}^j(zs) = \epsilon^{ij} x_{10}^2\, I_4(x_{10}^2, zs) + \epsilon^{ik} x_{10}^k x_{10}^j\, I_5(x_{10}^2, zs) + \epsilon^{jk} x_{10}^k x_{10}^i\, I_6(x_{10}^2, zs) \dots. \tag{9b}$$

Note other tensor structures are possible in Eqs. (8b) and (9), as indicated by the ellipses, but they do not contribute to the OAM distributions so we disregard them here. The functions I_3, I_4, I_5, I_6 were dubbed the "moment" amplitudes in [3].

To obtain the OAM distributions at small-x, we substitute Eqs. (5) in Eq. (4) and expand in x. The leading non-trivial terms can be expressed in terms of the impact-parameter integrated amplitudes of Eqs. (8) and (9). The resulting OAM distributions are then

$$L_{q+\bar{q}}(x, Q^2) = \frac{N_c N_f}{2\pi^3} \int\limits_{\Lambda^2/s}^{1} \frac{dz}{z} \int\limits_{\frac{1}{zs}}^{\min\left[\frac{1}{zQ^2}, \frac{1}{\Lambda^2}\right]} \frac{dx_{10}^2}{x_{10}^2} \left[Q - 3\, G_2 - I_3 - 2\, I_4 + I_5 + 3\, I_6\right](x_{10}^2, zs), \tag{10a}$$

$$L_G(x, Q^2) = -\frac{2N_c}{\alpha_s \pi^2} \left[2\, I_4 + 3\, I_5 + I_6\right]\left(x_{10}^2 = \frac{1}{Q^2},\, zs = \frac{Q^2}{x}\right), \tag{10b}$$

where Λ is an infrared (IR) cutoff. Eqs. (10) are derived in the double logarithmic approximation (DLA), which resums powers of $\alpha_s \ln^2(1/x)$. To determine the small-x asymptotics of the OAM distributions, we first need to evolve the amplitudes in Eqs. (8) and (9). Although the evolution equations for $Q(x_{10}^2, zs)$ and $G_2(x_{10}^2, zs)$ were derived in [1], we still need to derive evolution equations for the moment amplitudes, I_3, I_4, I_5, I_6.

3. Moment amplitude evolution equations in the large-N_c limit

The polarized dipole amplitudes in Eqs. (7) can be evolved partonic center of mass energy zs [1]. Similar to the Balitsky hierarchy in unpolarized scattering [12, 13], these evolution equations do not close in general. However, they do close in the large-N_c limit. The evolution equations for $G_{10}(zs)$ (which is the notation for $Q_{10}(zs)$ in the large-N_c limit) and $G_{10}^i(zs)$ are given by Eqs. (118) and (128) of [1], respectively. Starting with these equations, one can multiply both sides by a factor of x_1^m and integrate over x_1. Keeping only leading terms in the DLA, we derive the large-N_c evolution equations for the moment amplitudes in Eqs. (9). The result, derived in [3], is

$$\begin{pmatrix} I_3 \\ I_4 \\ I_5 \\ I_6 \end{pmatrix}(x_{10}^2, zs) = \begin{pmatrix} I_3^{(0)} \\ I_4^{(0)} \\ I_5^{(0)} \\ I_6^{(0)} \end{pmatrix}(x_{10}^2, zs) + \frac{\alpha_s N_c}{4\pi} \int\limits_{\frac{1}{sx_{10}^2}}^{z} \frac{dz'}{z'} \int\limits_{\frac{1}{z's}}^{x_{10}^2} \frac{dx_{21}^2}{x_{21}^2} \begin{pmatrix} 2\,\Gamma_3 - 4\,\Gamma_4 + 2\,\Gamma_5 + 6\,\Gamma_6 - 2\,\Gamma_2 \\ 0 \\ 0 \\ 0 \end{pmatrix}(x_{10}^2, x_{21}^2, z's) \tag{11}$$

$$+\frac{\alpha_s N_c}{4\pi}\int_{\frac{\Lambda^2}{s}}^{z}\frac{dz'}{z'}\int_{\max[x_{10}^2,\frac{1}{z's}]}^{\min[\frac{z}{z'}x_{10}^2,\frac{1}{\Lambda^2}]}\frac{dx_{21}^2}{x_{21}^2}\begin{pmatrix}4&-4&2&6&-4&-6\\0&4&2&-2&0&1\\-2&2&-1&-3&2&3\\0&0&0&0&2&4\end{pmatrix}\begin{pmatrix}I_3\\I_4\\I_5\\I_6\\G\\G_2\end{pmatrix}(x_{21}^2,z's).$$

The neighbor amplitudes[2] $\Gamma_3,\Gamma_4,\Gamma_5,\Gamma_6$ obey their own evolution equations, given in Eq. (54f) of [3]. The evolution equations for G, G_2, and Γ_2 are given in Eq. (133) of [1]. An important feature of our Eq. (11) is the mixing of the moment amplitudes with the dipole amplitudes G and G_2. A similar mixing between helicity and orbital sectors can be found in the DGLAP evolution equations for the twist-2 part of the OAM distributions [14, 15].

4. Numerical Results

We can solve Eq. (11) numerically. From the form of Eq. (11), we see that it is more convenient to work with the logarithmic variables

$$s_{10}=\sqrt{\frac{\alpha_s N_c}{2\pi}}\ln\frac{1}{x_{10}^2\Lambda^2},\qquad \eta=\sqrt{\frac{\alpha_s N_c}{2\pi}}\ln\frac{zs}{\Lambda^2}. \tag{12a}$$

At large η and fixed s_{10}, the moment amplitudes $I_3(s_{10},\eta)$, $I_4(s_{10},\eta)$, $I_5(s_{10},\eta)$,and $I_6(s_{10},\eta)$ seem to grow exponentially (see Figure 1 of [3]). Therefore, we have the following ansatz[3],

$$I_p(s_{10}=0,\eta)\sim\exp\left[\alpha_{I_p}\eta\sqrt{\frac{2\pi}{\alpha_s N_c}}\right], \tag{13}$$

where $p=3,4,5,6$ and α_{I_p} is the intercept. We regress a linear model on $\ln|I_p(s_{10}=0,\eta)|$ to fit the intercept. However, this can only be done at finite step sizes in η. To approximate the continuum limit, we repeat this procedure at different step sizes $\delta=\Delta\eta$ and maximum η values ($\eta_{\max}$), obtaining a surface in the $(\delta,1/\eta_{\max})$ space. We then fit this surface to a polynomial model to extract the continuum limit $(\delta,1/\eta_{\max}\to 0)$ intercept [1, 16]. The resulting intercepts for the moment amplitudes are all numerically consistent,

$$\alpha_{I_3}=\alpha_{I_4}=\alpha_{I_5}=\alpha_{I_6}=3.66\sqrt{\frac{\alpha_s N_c}{2\pi}}. \tag{14}$$

Using Eq. (14) along with Eq. (13) in Eqs. (10), we determine the small-x, large-N_c asymptotics of the OAM distributions to be

$$L_{q+\bar{q}}(x,Q^2)\sim L_G(x,Q^2)\sim\left(\frac{1}{x}\right)^{3.66\sqrt{\frac{\alpha_s N_c}{2\pi}}}. \tag{15}$$

The helicity PDFs, $\Delta\Sigma(x,Q^2)$, $\Delta G(x,Q^2)$ and the g_1 structure function have the same asymptotics as Eq. (15) [1]. Therefore, from Eq. (15) we conclude that the OAM distributions are not suppressed relative to the helicity distributions at small x.

[2]The so-called neighbor amplitudes are auxiliary functions necessary to enforce lifetime ordering in the evolution [11]. They do not contribute directly to the OAM distributions or the helicity PDFs.

[3]The factor $\sqrt{\frac{2\pi}{\alpha_s N_c}}$ is due to the definition of η in Eq. (12).

Another important quantity to investigate beyond the small-x asymptotics is the ratio of the OAM distributions to the helicity PDFs. Using the numerical solution of Eqs. (11), we can calculate the OAM distributions via Eqs. (10). Similarly, we perform a numerical solution of the helicity evolution equations, Eq. (133) of [1], to obtain the helicity PDFs via Eqs. (42) and (66) of [1]. In Figure 1, we plot the ratio of the quark OAM distribution to the quark helicity PDF in panel (a) and the ratio of the gluon OAM distribution to the gluon helicity PDF in panel (b) as a function of $\ln(1/x)$.

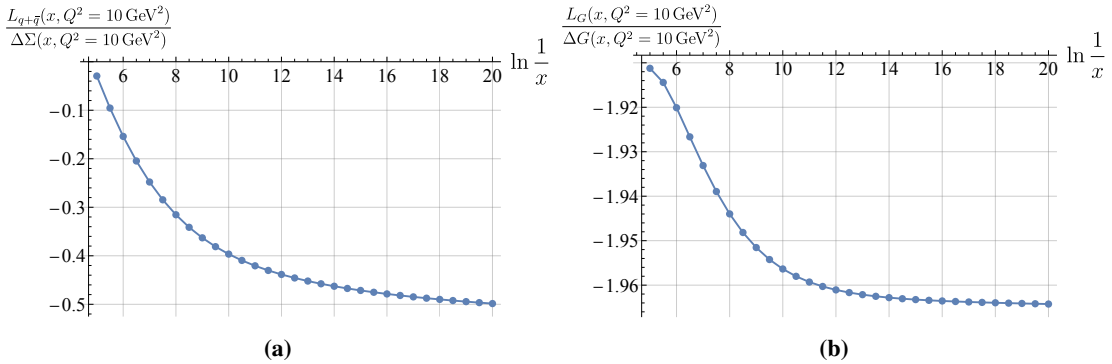

Figure 1: Plots of the OAM to helicity PDF ratios from Eqs. (16) in the quark (a) and gluon (b) sector as a function of $\ln(1/x)$. Here $Q^2 = 10\,\mathrm{GeV}^2$, $N_c = 3$, $\alpha_s = 0.25$, and the step size is $\Delta\ln(1/x) = 0.5$.

From Figure 1, we get the following ansätze for the ratios

$$\frac{L_{q+\bar{q}}(x,Q^2)}{\Delta\Sigma(x,Q^2)} = A_q + \frac{B_q}{\ln\frac{1}{x}}, \tag{16a}$$

$$\frac{L_G(x,Q^2)}{\Delta G(x,Q^2)} = A_G + \frac{B_G}{\ln\frac{1}{x}}. \tag{16b}$$

The form of these ansätze are justified in the Appendix of [3]. We can fit the ratios in Figure 1 to the ansätze of Eqs. (16) for a given step size in x. By performing a similar procedure to the one outlined above for the small-x asymptotics, we can obtain estimates for the ratio coefficients in Eqs. (16) in the continuum limit. For $Q^2 = 10\,\mathrm{GeV}^2$, the numerically-determined coefficients are

$$\frac{L_{q+\bar{q}}(x,Q^2)}{\Delta\Sigma(x,Q^2)} = -(0.5698 \pm 0.0002) + \frac{(1.31 \pm 0.01)}{\ln\frac{1}{x}}, \tag{17a}$$

$$\frac{L_G(x,Q^2)}{\Delta G(x,Q^2)} = -(1.96657 \pm 0.00003) + \frac{(0.0531 \pm 0.0002)}{\ln\frac{1}{x}}. \tag{17b}$$

We should compare Eqs. (17) to the results obtained in [2]. For helicity PDFs with small-x asymptotics

$$\Delta\Sigma(x,Q^2), \Delta G(x,Q^2) \sim \left(\frac{1}{x}\right)^{\alpha}, \tag{18}$$

Eq. (7) of [2] predicts

$$L_{q+\bar{q}}(x,Q^2) = -\frac{1}{1+\alpha}\Delta\Sigma(x,Q^2) \approx -\Delta\Sigma(x,Q^2), \tag{19a}$$

$$L_G(x,Q^2) = -\frac{2}{1+\alpha}\Delta G(x,Q^2) \approx -2\,\Delta G(x,Q^2), \tag{19b}$$

where, in the last equality, we expanded in the perturbatively small parameter $\alpha \sim \sqrt{\alpha_s}$. Comparing Eqs. (17) and Eqs. (19), we see that the quark ratios are different by nearly 50% and the gluon ratios are nearly consistent. Although some speculation on the discrepancy in the quark ratio can be found in [3], so far, there is no clear answer as to why the two results differ. We expect the analytic solution of Eq. (11) will shed light on this matter. One potential source of this discrepancy is the Wandzura-Wilczek (WW) approximation employed in [2]. The WW approximation keeps only the twist-2 contributions to the OAM distributions. While not explicitly identified, the twist-3 contributions to the OAM distributions are not neglected here (or in the full work [3]). See the discussion below Eqs. (71) in [3] for more details.

5. Conclusions and Outlook

To conclude, we have studied the OAM distributions at small x. By including corrections to the sub-eikonal evolution found in [1], we revised and updated the results of [8]. We were able to relate the OAM distributions to the polarized dipole amplitude and their first impact-parameter moments (the moment amplitudes), exhibited in Eqs. (10). We have derived new large-N_c evolution equations for the moment amplitudes and solved them numerically. The numerical solution revealed that the OAM distributions have the same small-x asymptotics as the helicity PDFs and g_1 structure function, shown in Eq. (15), in agreement with [2].

We also studied the ratio of the OAM distributions to the helicity PDFs in the small-x region. In the quark sector, we found a discrepancy with [2], while in the gluon sector we found agreement. A more in depth discussion of all the points listed above can be found in the full work, [3].

Acknowledgments

The author would like to thank Yuri Kovchegov for collaborating on this project, and Josh Tawabutr for helpful discussions and for generously making his code for the helicity evolution available to him. This material is based upon work supported by the U.S. Department of Energy, Office of Science, Office of Nuclear Physics under Award Number DE-SC0004286 and is performed within the framework of the Saturated Glue (SURGE) Topical Theory Collaboration.

References

[1] F. Cougoulic, Y.V. Kovchegov, A. Tarasov and Y. Tawabutr, *Quark and gluon helicity evolution at small x: revised and updated*, *Journal of High Energy Physics* **2022** (2022) .

[2] R. Boussarie, Y. Hatta and F. Yuan, *Proton Spin Structure at Small-x*, *Phys. Lett.* **B797** (2019) 134817 [1904.02693].

[3] Y.V. Kovchegov and B. Manley, *Orbital Angular Momentum at Small x Revisited*, 2310.18404.

[4] R.L. Jaffe and A. Manohar, *The G(1) Problem: Fact and Fantasy on the Spin of the Proton*, *Nucl. Phys.* **B337** (1990) 509.

[5] C. Lorce and B. Pasquini, *Quark Wigner Distributions and Orbital Angular Momentum*, *Phys. Rev.* **D84** (2011) 014015 [1106.0139].

[6] C. Lorce, B. Pasquini, X. Xiong and F. Yuan, *The quark orbital angular momentum from Wigner distributions and light-cone wave functions*, *Phys. Rev.* **D85** (2012) 114006 [1111.4827].

[7] X. Ji, X. Xiong and F. Yuan, *Probing Parton Orbital Angular Momentum in Longitudinally Polarized Nucleon*, *Phys. Rev.* **D88** (2013) 014041 [1207.5221].

[8] Y.V. Kovchegov, *Orbital Angular Momentum at Small x*, *JHEP* **03** (2019) 174 [1901.07453].

[9] P.J. Mulders and R.D. Tangerman, *The Complete tree level result up to order 1/Q for polarized deep inelastic leptoproduction*, *Nucl. Phys.* **B461** (1996) 197 [hep-ph/9510301].

[10] Y.V. Kovchegov and M.D. Sievert, *Small-x Helicity Evolution: an Operator Treatment*, *Phys. Rev.* **D99** (2019) 054032 [1808.09010].

[11] Y.V. Kovchegov, D. Pitonyak and M.D. Sievert, *Helicity Evolution at Small-x*, *JHEP* **01** (2016) 072 [1511.06737].

[12] I. Balitsky, *Operator expansion for diffractive high-energy scattering*, *AIP Conf. Proc.* **407** (1997) 953 [hep-ph/9706411].

[13] I. Balitsky, *Factorization and high-energy effective action*, *Phys. Rev.* **D60** (1999) 014020 [hep-ph/9812311].

[14] P. Hagler and A. Schafer, *Evolution equations for higher moments of angular momentum distributions*, *Phys. Lett.* **B430** (1998) 179 [hep-ph/9802362].

[15] P. Hoodbhoy, X. Ji and W. Lu, *Quark orbital-angular-momentum distribution in the nucleon*, *Physical Review D* **59** (1998) .

[16] Y.V. Kovchegov, D. Pitonyak and M.D. Sievert, *Small-x asymptotics of the quark helicity distribution*, *Phys. Rev. Lett.* **118** (2017) 052001 [1610.06188].